Evaluation Method of Spherical Marker Arrangement for LiDAR-SLAM using a Robot Simulator

Tomoki Sugihara [1]*, Rikako Shigefuji[1] , Keitaro Kitamura[2] , Masanori Takigawa[2] , Takahiro Hiramatu[2] , Taizo Kobayashi[3] , Masafumi Nakagawa[1]

[1]First Author's Affiliation: Shibaura Institute of Technology, Japan

[2]Second Author's Affiliation: Asia Air Survey Co., Ltd., Japan

[3]Third Author's Affiliation: Ritsumeikan University, Japan

*ah20086@shibaura-it.ac.jp (*Corresponding author's email only)

Abstract: *Recently, the Ministry of Land, Infrastructure, Transport and Tourism (MLIT) has been promoting a project to develop innovative unmanned construction technologies for construction activities on the Lunar and other bodies in the Space Unmanned Construction Innovation Technology Development and Promotion Project. The purpose of this project is not only to promote the world's first lunar base construction, but also to further advance and disseminate unmanned construction technologies to the field and spread them to projects on the ground to cope with increasingly severe disasters, national land resilience, and a declining population. This has stimulated discussion on the technological development of lunar base construction. The development of unmanned surveying and remote construction technologies is essential for ground surveying in the initial phase of a lunar base construction project. However, due to the extreme temperature changes and space radiation in the lunar environment, it is difficult to conduct conventional surveying using a total station (TS) as is done on the Earth. In addition, Simultaneous Localization and Mapping (LiDAR-SLAM) using conventional LiDAR is not suitable for measurement in a non-GNSS environment and in microtopography with poor geometric features where reference points are not well developed, and one surface is covered with regolith. Simultaneous Localization and Mapping (LiDAR-SLAM), which uses conventional LiDAR, is not suitable for measurement in microtopography. Therefore, the application of LiDAR-SLAM that uses spherical markers as landmarks is considered to be suitable for topographic measurements on the Lunar. However, the optimization of marker placement planning has not yet been studied and remains an issue. Therefore, it is essential to obtain basic data on the relative positional relationship between the spherical marker and LiDAR in marker extraction. In this study, we propose a method for evaluating the placement of spherical markers used in LIDAR-SLAM by using a robot simulator to reproduce an experimental field that imitates the surface of the lunar.*

Keywords: LiDAR, Simulator, Unmanned Surveying

Introduction

In recently years, the Ministry of Land, Infrastructure, Transport and Tourism (MLIT) has been promoting a project to develop innovative unmanned construction technologies for construction activities on the lunar and other bodies in the Space Unmanned Construction Innovative Technology Development Promotion Project. MLIT considers remote or automated construction technology (e.g., unmanned construction) to be an important element for constructing the world's first lunar base for space exploration, and states that Japan's unmanned construction technology, which has overcome many disasters in the past, is an international strength. In addition, to strengthen the national land preparedness against disasters that have become more severe in recent years and to cope with the decrease in the working population due to population decline, the project aims to further advance and disseminate unmanned construction technology at construction sites, develop technology to adapt to lunar base construction, and extend the technology to projects on the surface of the lunar. This has stimulated the development of lunar base construction technology. The development of unmanned surveying and remote construction technologies is essential for ground surveying in the initial phase of a lunar base construction project. However, the lunar environment is subject to extreme temperature changes and cosmic radiation, making conventional surveying using a TS difficult, as is the case on Earth. In addition, the lunar surface is covered entirely by regolith, which is a microtopography that is achromatic and lacks image and shape features. Therefore, Simultaneous Localization and Mapping (LiDAR-SLAM) using conventional LiDAR and Visual-SLAM using cameras are not suitable. Therefore, LiDAR-SLAM, which uses spherical markers as landmarks, is considered to be suitable for topographic measurements on the lunar, and research is underway. However, the optimization of marker placement planning has not been studied yet, and this is an issue. In this study, we propose an evaluation method of spherical marker placement for LiDAR-SLAM by using a robot simulator to reproduce an experimental field that imitates the lunar surface.

Literature Review

Two papers are mentioned as existing research. The first is a paper on the validation of SLAM and self-positioning estimation methods for autonomous remote construction on the lunar (Hamamoto et al., 2023). Unlike on Earth, the lunar environment has significantly different gravity and soil conditions, making it difficult to apply conventional terrestrial construction techniques as they are. Therefore, based on the lunar base construction scenario proposed by the JAXA International Space Exploration Centre, technological verification of excavation work in an environment simulating the lunar surface was carried out. In particular, the effectiveness of SLAM technology in an environment where GNSS (Global Navigation Satellite System) is not available, co-operative control between multiple automated construction machines, and integrated technology for remote control and automatic control are examined. The lunar surface has few feature points, which may cause degeneracy problems with ordinary LiDAR-SLAM. It has been confirmed that mapping and self-position estimation can be performed correctly to a certain degree while avoiding degeneration by installing a temporary enclosure. It has also been confirmed that Visual-SLAM is effective when used in environments where it is difficult for LiDAR-SLAM to capture them as feature points. Second, there is a study on the acquisition of high-density point clouds using LiDAR-SLAM and SfM/MVS in the lunar environment. Conventional LiDAR-SLAM has the problem that it is difficult to be applied in an environment with poor geometrical features such as the lunar surface (Shigefuji et al., 2023). On the other hand, SfM/MVS is superior in generating high-resolution 3D models, but its scaling uncertainties and lack of real-time performance have been considered as challenges. We propose a data acquisition method that integrates these technologies and is suitable for the lunar environment, using JAXA's lunar exploration field as a test site to acquire data from LiDAR on board the lunar rover and from cameras placed on the spherical markers. First, a point cloud was generated from the images acquired by the high-resolution camera using SfM/MVS. Subsequently, LiDAR and AHRS are combined to correct the acquired point cloud and perform scaling based on the marker positions. Finally, the point cloud is matched with the point cloud of the spherical marker obtained by LiDAR-SLAM to obtain a point cloud with high density, scale and color information. Experimental results confirm that the red sphere markings are effective for both LiDAR-SLAM and SfM/MVS and enable highly accurate point cloud acquisition in the lunar environment. However, the optimization of the marker placement plan has not yet been investigated and remains a challenge.

Methodology

The proposed method in this study is shown in Figure 1. First, a time-series LiDAR point cloud that reflects gimbal rotation is combined to reproduce a point cloud of 360° around the LiDAR. Next, only spherical point clouds are extracted from the acquired point clouds, and multiple spherical point clouds are classified one by one by a clustering process. For each cluster, model fitting of the spherical point clouds is performed to estimate the location of the center of the marker from the point clouds on the marker surface. The residuals in the estimation are used to evaluate whether the required accuracy is met or not, and the maximum distance between the LiDAR and the spherical marker that meets the required accuracy can be calculated. Then, we randomly place spherical markers within the range of the maximum distance that satisfies the required accuracy and within the range of 30° to 150° of foreign angle between the markers as seen from LiDAR. After that, multiple patterns of marker placement are created, and whether the rover's self-position estimation accuracy meets the required accuracy is evaluated based on the backward crossing method. By attaching an error to the center position of the marker in advance, the impact of the included angles on the accuracy of self-position estimation is quantitatively assessed.

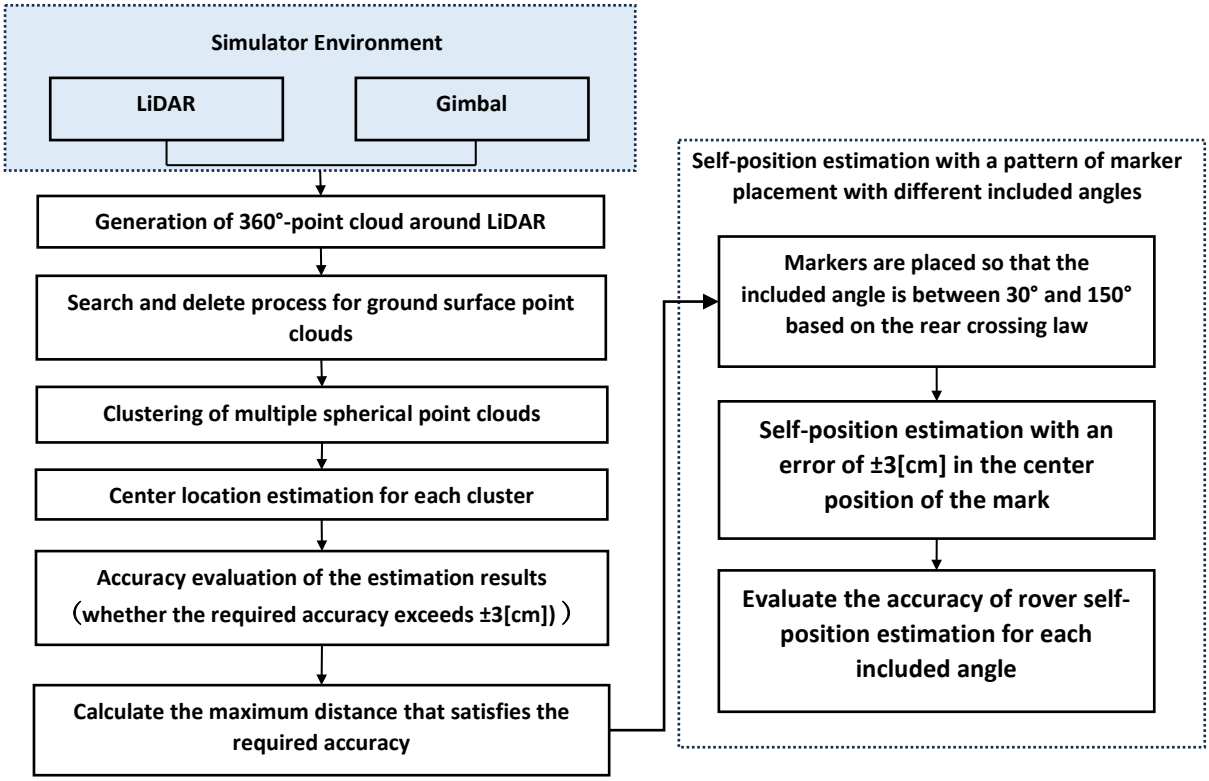

Figure 1: Evaluation method for placement of spherical markers.

a. Generation of 360°-point cloud centered on LiDAR:

In this study, a gimbal is mounted on a rover in a robot simulator environment, and LiDAR is attached to the gimbal to acquire point clouds while rotating the gimbal (Figure2). The same rotation angle resolution of the gimbal used in the real-space experiment is set for the gimbal in the robot simulator environment to ensure consistency between the experimental environment and the simulation environment. In addition, since the center of LiDAR and the rotation axis of the gimbal are misaligned by several centimeters in the x-axis and y-axis, respectively, offset correction of the rotation axis is performed to account for this. The point clouds acquired during one rotation of the gimbal are then superimposed to generate a high-density point cloud of 360 degrees around the LiDAR.

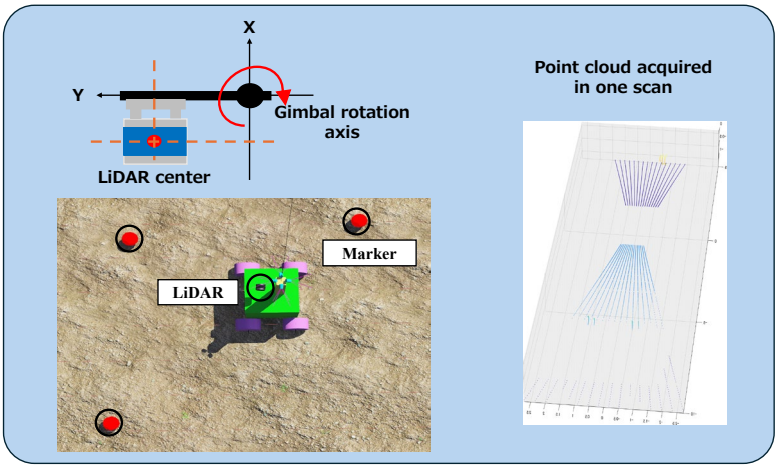

Figure 2: point cloud coupling process.

b. Estimation of the center position of a spherical Marker:

The point cloud of the ground surface is estimated from the point cloud of 360° around the LiDAR. Only spherical point clouds are extracted by calculating the point with the highest value in the Z-axis direction from the point clouds extracted as the ground surface and deleting the point clouds with a value lower than that value. The extracted spherical point clouds are further classified into spherical point clouds one by one by means of a clustering process. The extracted point clouds may also include cylindrical poles used as marker posts and point clouds on the ground surface that could not be processed. Therefore, segmentation is performed so that only spherical point clouds are extracted. ICP is used to find the nearest neighbor points in the other point cloud for each point in one point cloud, and to map these points to the corresponding points in the other point cloud. The ICP then estimates the rigid-body transformation matrix that minimizes the distance between the corresponding points. The two point clouds are then aligned by

repeating the mapping and rigid-body transformation estimation. However, if the initial positions of the two point clouds are far apart, the alignment fails, which means that the initial positioning of the two point clouds has a significant impact on the fitting accuracy in ICP. Therefore, in this study, the center of gravity of each spherical point cloud is calculated and the position of the center of gravity is set as the initial position of the spherical model to improve the fitting accuracy. In ICP, if a 3D sphere model is used as the reference model, a complex algorithm is required to search for the corresponding points, and it is difficult to improve the accuracy because of the different data format. A hemispheric model is used as the reference model. The reason is that if a global model is used for model fitting, the extracted spherical point cloud may not fit well along the spherical surface as shown in Figure 3, resulting in a large error in center position estimation.

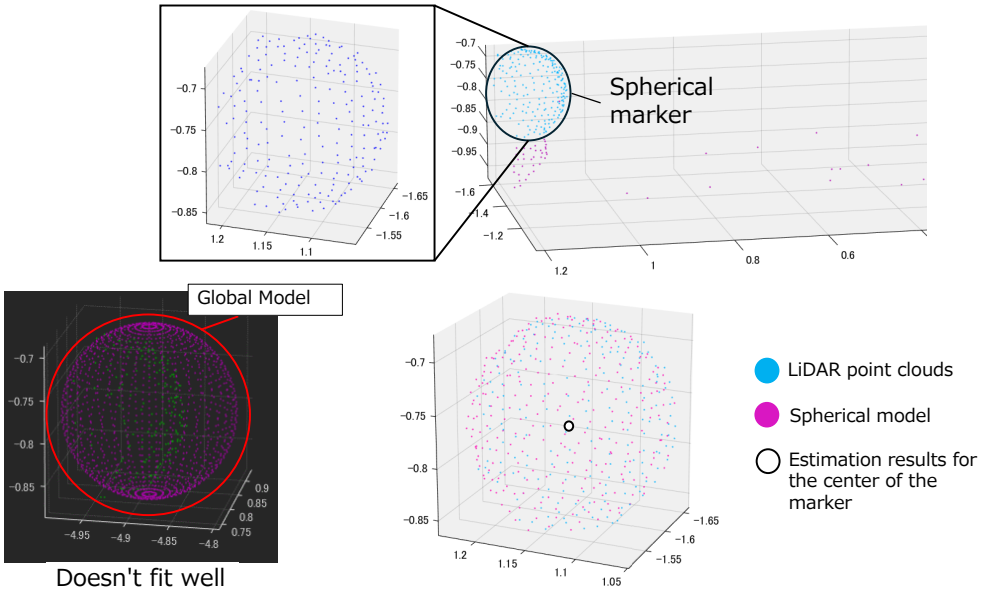

Figure 3: Marker extraction and center location estimation.

c. Self-position estimation using the backward crossing method:

The rover's self-position estimation is based on the backward crossing method, which is solved analytically using the values of three reference points. First, the coordinates of the center of the marker are used as reference points, as shown in Figure 4. The rover's self-position is treated as known information, and the radius of each circle is calculated by drawing three circles with the line connecting the center of the marker and the rover's self-position as the radius. The intersection points where the three circles intersect is then evaluated for accuracy as the estimated value of the rover's self-position. The coordinates of the center of the marker are given an arbitrary error value that is equivalent to the

ranging accuracy of LiDAR, and the degree of influence of the angle measurement determined by the relative positional relationship between the rover and the marker is evaluated by estimating the rover's self-position for each foreign angle.

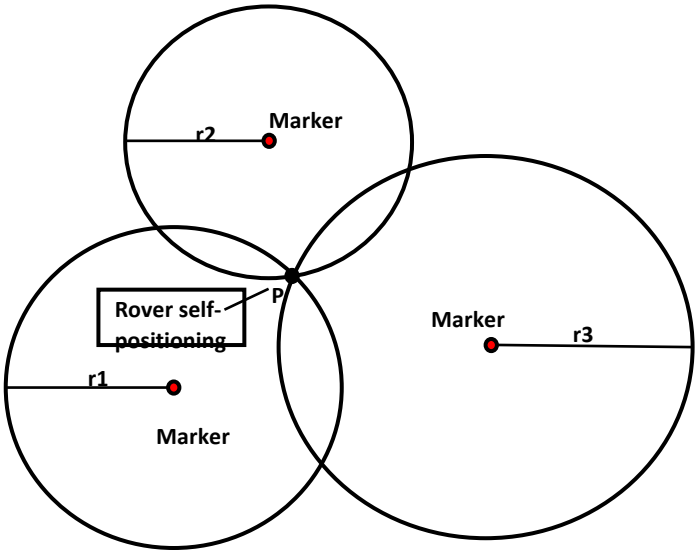

Figure 4: Self-position estimation using arcs.

Experiments

The experiment was conducted in an experimental field (Biwako Kusatsu Campus, Ritsumeikan University) (Figure 5) that imitated the surface of the lunar. Red spherical markers with a diameter of 0.20 [m] were randomly placed at 14 locations outside the field, and the field was divided into five lanes, with the rover stopping at seven locations per lane to acquire a point cloud at each location. LiDAR (VLP-16, Velodyne) (Table 1) and AHRS (MTi-G-710, Xsens) mounted on gimbals inclined 90° from the horizontal plane were mounted on the rover, and the gimbals were rotated 360° horizontally at any stop position for an all-surrounding scan by a smartphone application. The rover was remotely controlled by a smartphone app. Furthermore, the field experiment site was reproduced in a simulator (Webots) and the experiment was conducted under conditions similar to those in the real environment (Figure 6). At this time, it was not possible to reproduce detailed terrain and geographical features such as irrigation channels, trees and tents around the field. As the robot simulator could not create a gimbal for use in real space, a method was adopted to reproduce the point cloud that can be acquired by the combination of gimbal and LiDAR by setting the position and rotation angle of the rotation axis and rotating the LiDAR. In order to verify whether the marker placement using the backward crossing method is applicable, several marker placement patterns with different foreign angle were prepared and the rover's self-position (in this study, the center position of the LiDAR) was

estimated for each pattern. The markers were placed so that the maximum distance between the LiDAR and the markers satisfied the required accuracy (Figure 7).

Table 1. LiDAR performance used in the experiments.

LiDAR(VLP-16, Velodyne)	
Distance measurement accuracy	3cm
Angle resolution(Horizaontal axis)	0.25 deg
Angle resolution(Vertical axis)	2 deg
Measurement range(Horizontal axis)	360 deg
Measurement range(Vertical axis)	±15 deg
Sampling rate	10 Hz

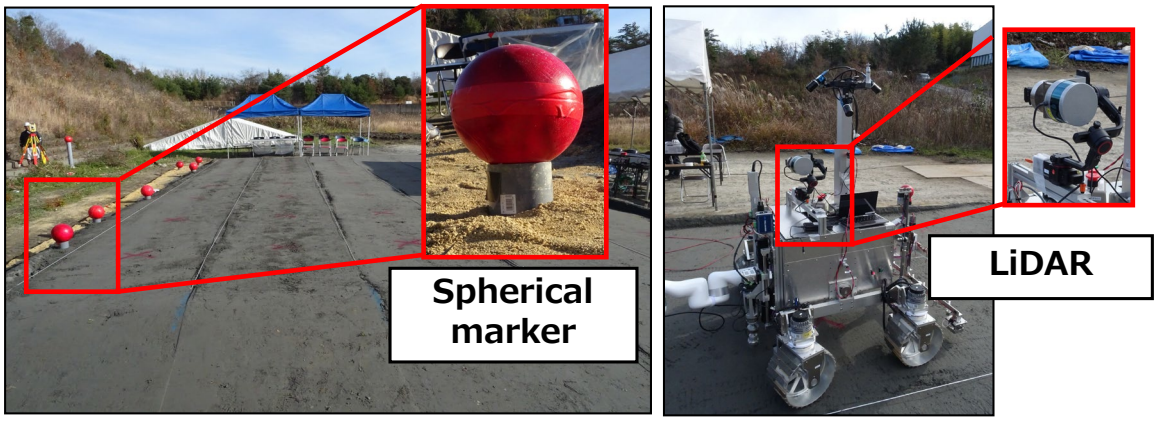

Figure 5: Experimental site and LiDAR（VLP,Velodyne） and marking used.

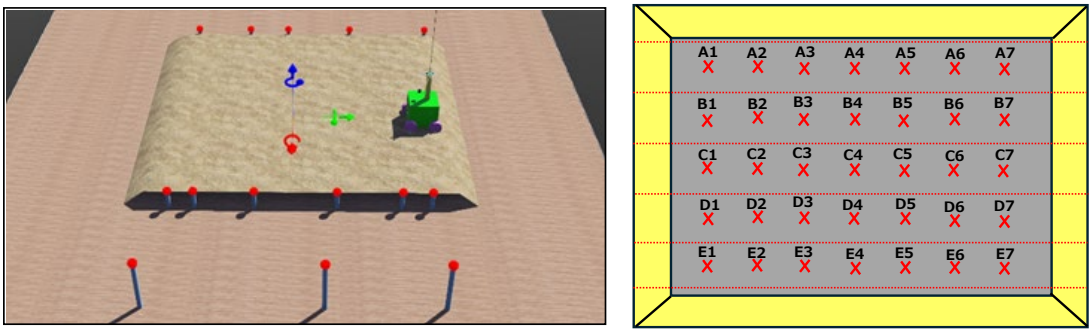

Figure 6: Simulator environment reproducing the actual experimental environment and the rover's stopping position.

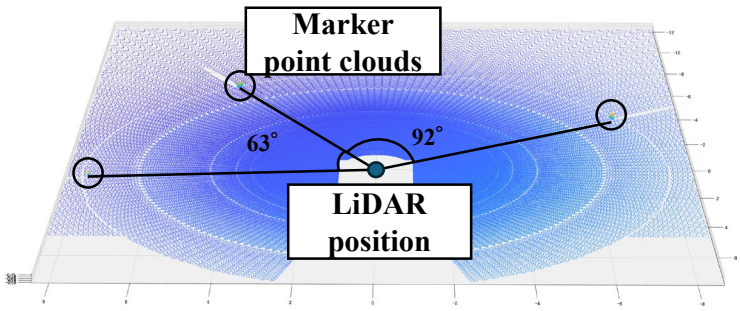

Figure 7: Marker placement considering the included angle.

Results

In the simulation experiments, the distance between LiDAR and the center position of the spherical marker was calculated and the accuracy of the marker center position estimation for each distance is shown in Table 2. The foreign angle was calculated from the center position of the sphere marker and the rover's self-position, and the results of the self-position estimation accuracy for each foreign angle are summarized in Table 2. The self-position estimation errors in Table 3 show the relative accuracy based on the theoretical value of the position estimation of the center of the marker for each foreign angle. The self-position estimation errors are color-coded red and blue, based on a required accuracy of ±3 cm. Table 4 shows the average estimation error calculated from the point cloud of spherical markers acquired at seven locations on sideline 2, for each location, the center position of all markers was calculated, and the average estimation error was calculated and tabulated.

Table2: Estimation accuracy of marker center location by distance.

Distance between LiDAR and marker[m]	Number of point cloud	Presumed center position of marker			Estimation accuracy
		X[m]	Y[m]	Z[m]	
6.84	142	-0.0084	-0.0193	-0.0140	0.0253
7.15	130	0.0068	0.0119	0.0156	0.0208
7.19	150	0.0012	-0.0244	-0.0118	0.0271
7.71	107	0.0300	0.0079	0.0208	0.0374
7.76	122	0.0222	0.0074	0.0155	0.0281
7.84	119	0.0016	-0.0226	-0.0166	0.0281
7.90	96	0.0007	0.0248	0.0094	0.0265
7.94	108	0.0067	0.0238	0.0137	0.0283
7.99	111	0.0130	0.0156	0.0125	0.0239
8.17	121	0.0022	0.0272	0.0049	0.0277
8.27	83	0.0186	0.0085	0.0187	0.0277
9.02	80	0.0266	0.0271	0.0222	0.0438
9.13	68	0.0048	0.0229	0.0130	0.0268
9.34	93	0.0153	0.2920	0.0186	0.0379

Table3: Accuracy of self-position estimation for each included angle.

Process ID	Included angle[°]	center-of-marker estimation			Granted error[m]	Self-position estimation error[m]
		X[m]	Y[m]	Z[m]		
1	17.54	±0.017	±0.017	±0.017	0.030	0.0560
2	33.19	±0.017	±0.017	±0.017	0.030	0.0350
3	57.54	±0.017	±0.017	±0.017	0.030	0.0277
4	99.27	±0.017	±0.017	±0.017	0.030	0.0256
5	133.13	±0.017	±0.017	±0.017	0.030	0.0284
6	148.59	±0.017	±0.017	±0.017	0.030	0.0324
7	165.05	±0.017	±0.017	±0.017	0.030	0.0477

Process ID	Included angle[°]	Distance measurement[m]		Granted error[m]	Self-position estimation error[m]
		Marker1	Marker2		
1	17.54	7.499	7.545	0.030	0.0560
2	33.19	7.499	7.527	0.030	0.0350
3	57.54	7.499	7.492	0.030	0.0277
4	99.27	7.499	7.537	0.030	0.0256
5	133.13	7.499	7.460	0.030	0.0284
6	148.59	7.499	7.403	0.030	0.0324
7	165.05	7.499	7.428	0.030	0.0477

Table4: Average center position estimation error per rover position.

sidetrack	position	average error[m]
B	1	0.0266
B	2	0.0222
B	3	0.0168
B	4	0.0160
B	5	0.0180
B	6	0.0208
B	7	0.0251

Discussion

The relationship between the center position estimation, the number of point clouds and the relative distance between the center position estimation and LiDAR in the simulation experiment is shown in Table 8. It can be seen that the accuracy of the center position estimation of the marker improves as the number of spherical point clouds increases. It can also be confirmed that the accuracy of the center position estimation worsens as the relative distance between the LiDAR and the marker increases. Based on this information, it was confirmed that an estimation accuracy of ±3 [cm], which is equivalent to the distance measurement accuracy of LiDAR, can be achieved for the accuracy of the center point of a marker if the distance between LiDAR and the marker is within 7.5 [m] and the number of spherical point clouds is more than 100 points. In the optimum placement of markers, it is desirable to keep the foreign angle in the range of 30° to 150° in the back crossing method, which is one of the conditions for the placement of markers. In this study, an error of ±0.03 [m] in estimating the position of the center of the marker was set as the given granted error. It was confirmed that the required accuracy of the rover's self-position estimation accuracy (±0.03 m) can be met by setting the foreign angle between 30° and 150° when the LiDAR and the marker are connected by a line. These results confirm that the marker placement considering the backward crossing method can be applied in a simulated lunar environment.

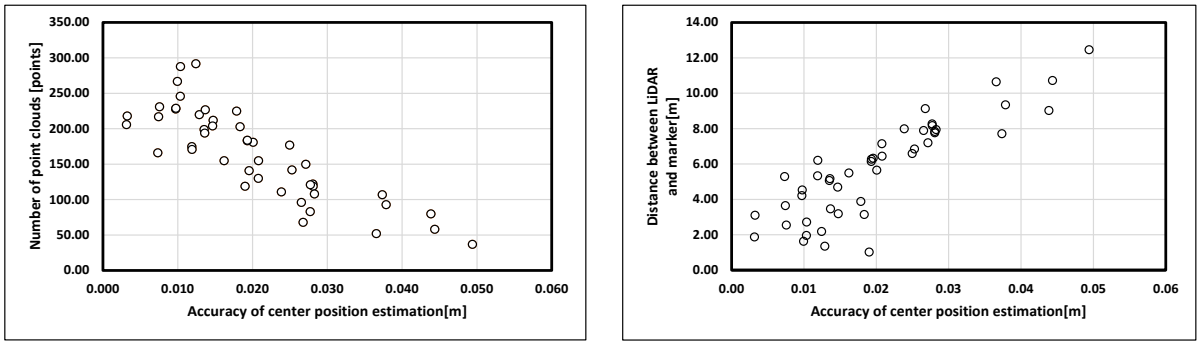

Figure8: Relationship between distance to mark vs. accuracy of center location estimation and relationship between number of point clouds and center location estimation.

a. Model fit-in influence of extracted spherical point clouds:

In this study, only spherical point clouds are extracted from the surrounding 360° point cloud centered on LiDAR to estimate the center position of them marker. The maximum value of the Z-axis in the ground surface point cloud is calculated, and all point clouds below that value are removed to eliminate poles, ground objects, and ground surface point clouds. At the same time, a portion of the spherical point cloud used for model fitting was also deleted, so the number of point clouds in the spherical point cloud is less than the number originally obtained (Figure 9). Experimental results confirm that a decrease in the number of spherical point cloud point clouds adversely affects the accuracy of center position estimation. In particular, the reduced number of point clouds results in insufficient data for model fitting, making it difficult to estimate the center position of the sphere at a level that meets the required accuracy. Furthermore, when the deleted point cloud included an even portion of the sphere surface, the fitting results became unstable, and the estimation error tended to increase. Based on these results, the focus in estimating the center position of a spherical point cloud is how to select the points to be deleted without reducing the number of spherical point clouds used for model fitting. Specifically, since the sequence of the point cloud is different between the cylinder pole portion and the spherical marker portion, a classification method using the difference in the sequence is considered to be suitable.

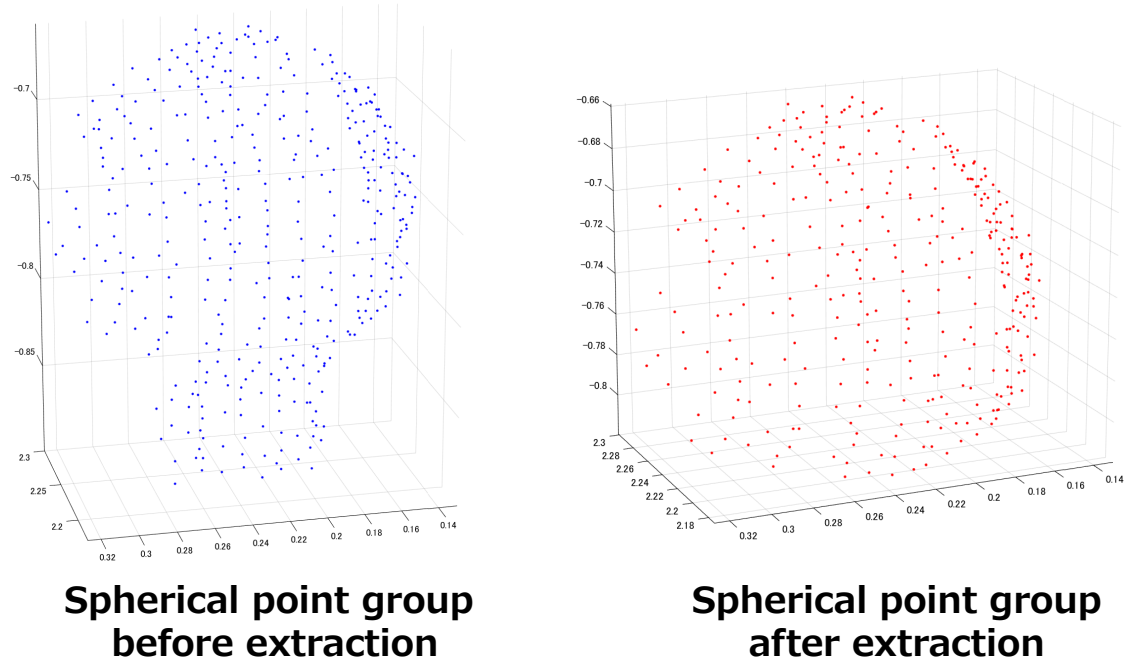

Figure9: Before and after the extraction process of spherical point clouds.

b. Influence of foreign angle on self-position estimation:

In the marker placement using the back crossing method, it was confirmed that the range of the rover's estimated self-position could be reduced by placing markers within the range of 30°~150° of the foreign angle. From Figure 10, it can be confirmed that the estimation error of the self-position estimation is about 0.03 [m] in the range of 30°~150°, but in the range of less than 30° or more than 150°, the estimation error is more than 0.03 [m]. This suggests that keeping within the range of 30°~150° will improve the accuracy of self-position estimation. Whilst angular constraints on the included angle of the marker arrangement are effective in improving position estimation accuracy, a non-linear multivariate analysis is required when rover measurements from multiple measurement positions are considered.

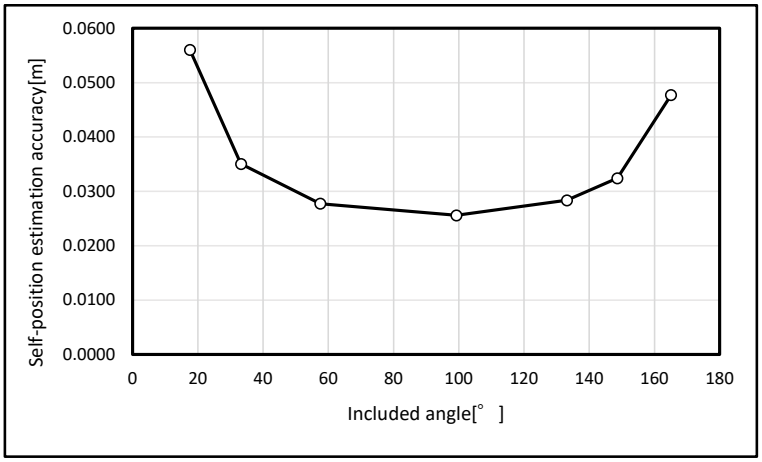

Figure10: Relationship between self-position estimation accuracy for each included angle.

c. Influence of foreign angle on self-position estimation:

From Figure 11, the average estimation error of the marker center position is the smallest at position 4, which is the center position of the lane, and the average estimation error increases as it approaches positions 1 and 7, which are the two ends of the lane, in acquiring the point cloud at seven locations per lane. From this, it can be said that the accuracy of the marker center position estimation increases as the rover approaches the center of the field in this study. It can also be confirmed that the relative distance between the LiDAR and the marker has an effect on the marker center position estimation.

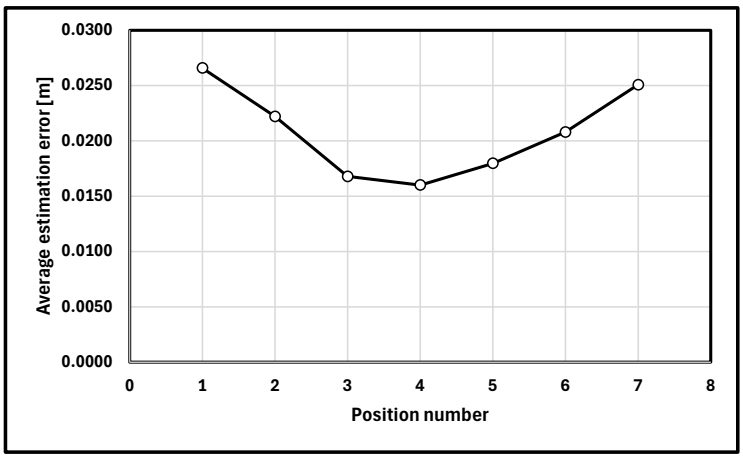

Figure11: Rover measurement position and mean center position estimation error.

Conclusion

In this study, an experimental field simulating the lunar surface is reproduced and a method for evaluating the placement of markers used in LiDAR-SLAM is proposed based on the results of the center position estimation of spherical markers. From the experimental results, it was confirmed that the required accuracy of within ±0.03 [m] was met when the distance between the LiDAR and the sphere markings was 7.5 [m] and the number of spherical points was 100 or more when VLP16 was used. It was also confirmed that the rover's self-position estimation accuracy can be kept within ±0.03[m] by setting the included angle in the back crossing method within the range of 30° to 150° when the accuracy of the marker center position estimation is about ±3[cm]. As this study did not reflect the results of the calibration of the gimbal rotation axis of the LiDAR, it is a future task to conduct experiments reflecting the results. Furthermore, when rover measurements from multiple measurement positions are considered, a non-linear multivariate analysis is considered necessary, as the placed markers may not be at the optimum distance or angle depending on the measurement position. In this case, the placement of the markers should also take into account the occlusion zone of the markers, and optimization is a challenge.

Acknowledgements

Ministry of Land, Infrastructure, Transport and Tourism and Ministry of Education, Culture, Sports, Science and Technology Stardust Program Ministry of Land, Infrastructure, Transport and Tourism (MLIT) and the Ministry of Education, Culture, Sports, Science and Technology (MEXT) Stardust Program. This is a part of the research on "Surveying and Geotechnical Investigation Methods for Creating 3D Geological Map of the Lunar Surface" under the Stardust Program of the Ministry of Land, Infrastructure, Transport and Tourism and the Ministry of Education, Culture, Sports, Science and Technology.

Reference

Kenichi Hamamoto, Yu Takagi, Shintaro Komatsu, Takahiro Ishikawa, Miura, Masataka Sudo, Yutaka Uchimura. (2023). Development of autonomous remote construction technology adapted to the construction environment - space application of next generation construction systems，Proceedings of the 67th Space Science and Technology Union.

Rikako Shigefuji, Karin Noguchi, Masanori Takigawa, Keitaro Kitamura, Takahiro Hiramatsu, Taizo Kobayashi, Masafumi Nakagawa. (2023). Acquisition of Dense Point Clouds with LiDAR-SfM/MVS Lunar Environment, Asian Conference on Remote Sensing (ACRS2023), p.6.

Ministry of Land, Infrastructure, Transport and Tourism, Space Unmanned Construction Innovative Technology Development Promotion Project. URL：https://www.mlit.go.jp/report/press/kanbo08_hh_000959.html，2024/03/26

Larry Matthies, Shreyansh Daftry, Scott Tepsuporn, Yang Cheng, Deegan Atha, R. Michael Swan Sanjna Ravichandar and Masahiro Ono. (2022). Lunar Rover Localization Using Craters as Landmarks, IEEE Aerospace Conference (AERO).

Liam Pedersen, Chin San Han, and Michael Vitus. (2008). Dark navigation: Sensing and rover navigation in permanently shadowed lunar craters, In International Symposium on Artificial Intelligence, Robotics and Automation in Space (ISAIRAS).

L. Pedersen, M. Allan, V. To, H. Utz, W. Wojcikiewicz, C. Chautems. (2010). High speed lunar navigation for crewed and remotely piloted vehicles, ISAIRAS, Sapporo, Japan.

Thrun, S., Montemerlo, M., and Aron, A. (2006). Probabilistic Terrain Analysis for High-Speed Desert Driving, Robotics Science and Systems Conference, Philadelphia.

S. Campbell, N. O'Mahony, A. Carvalho, L. Krpalkova, D. Riordan, and J. Walsh. (2020). "Where am I? localization techniques for mobile robots a review," in 2020 6th International Conference on Mechatronics and Robotics Engineering (ICMRE), IEEE, pp. 43-47.

Peng Li, Ruisheng Wang, Yanxia Wang, Wuyong Tao. (2020). Volume 8. Evaluation of the ICP Algorithm in 3D Point Cloud Registration, IEEE, pp.68030-68048.